NMR and Theoretical Study of Acidity Probes on Sulfated Zirconia Catalysts

James F. Haw,*,† Jinhua Zhang,§ Kiyoyuki Shimizu,† T. N. Venkatraman,† Donat-Pierre Luigi,† Weiguo Song,† Dewey H. Barich,§ and John B. Nicholas*,‡

Contribution from the Loker Hydrocarbon Research Institute and Department of Chemistry, University of Southern California, University Park, Los Angeles, California 90089-1661, the Environmental Molecular Sciences Laboratory, Pacific Northwest National Laboratory, P.O. Box 999, Richland, Washington 99352, and the Department of Chemistry, Texas A&M University, P.O. Box 300012, College Station, Texas 77842-3012

Received July 27, 2000. Revised Manuscript Received October 23, 2000

Abstract: The measurement of the type and number of acid sites on sulfated zirconia catalysts using the ^{31}P NMR spectrum of adsorbed $P(CH_3)_3$ has been vexed by spectral assignment controversies. Using a combination of NMR experiments and theoretical methods, including chemical shift calculations at the GIAO-MP2 level, we show that a previously observed ^{31}P resonance at +27 ppm is due to $P(CH_3)_4^+$, formed in a reaction that consumes a Brønsted site. The coproduct of this reaction, $PH(CH_3)_2$, is protonated on the surface to yield a ^{31}P resonance in the region expected for $P(CH_3)_3$ on a Lewis site. Further complications result from a signal due to $OP(CH_3)_3$, formed by oxidizing sites on the surface, complexed to unidentified acid sites. As an alternative, we show that carefully designed ^{15}N experiments using the less reactive and less basic probe pyridine-^{15}N provide more easily interpreted measurements of Brønsted and Lewis sites on sulfated zirconias of diverse composition, preparation, and treatment. Quantitative studies revealed that the number of Brønsted sites capable of protonating pyridine corresponded to only ∼7% of the sulfur atoms on the catalyst we studied in the greatest depth. Additional Brønsted sites were created on this catalyst with addition of water, a reaction not observed for sulfur-free zirconia.

Sulfated zirconia has attracted intense interest as a catalyst for alkane isomerization and related reactions at low temperatures. It is very active for the alkylation of butenes with butanes to form trimethylpentanes, for which thermodynamics mandates low temperatures to avoid dimethylhexanes—products with much lower octane numbers. Sulfated zirconia materials have motivated several recent reviews[1−5] and ongoing studies of their application and function.[6−13] Because low-temperature reactions of alkanes are also observed in superacid solutions, sulfated zirconia was early and frequently classified as a solid superacid, and this view persisted after similar views were overturned for zeolite solid acids.[14] The growing recognition that sulfated zirconia is also not a solid superacid[15] has removed the most convenient explanation for catalysis by this material and increased rather than diminished the need for fundamental study of this material.

Sulfated zirconia has been studied by theoretical methods[16,17] and spectroscopy,[18,19] including NMR.[20−26] It is undisputed that the surface of sulfated zirconia contains both Brønsted and Lewis acid sites, and much work has been carried out in attempts to

† University of Southern California.
‡ Pacific Northwest National Laboratory.
§ Texas A&M University.

(1) Song, X. M.; Sayari, A. *Catal. Rev.—Sci. Eng.* **1996**, *38*, 329−412.
(2) Adeeva, V.; Liu, H. Y.; Xu, B. Q.; Sachtler, W. M. H. *Top. Catal.* **1998**, *6*, 61−76.
(3) Yadav, G. D.; Nair, J. J. *Microporous Mesoporous Mater.* **1999**, *33*, 1−48.
(4) Cheung, T. K.; Gates, B. C. *Top. Catal.* **1998**, *6*, 41−47.
(5) Corma, A. *Chem. Rev.* **1995**, *95*, 559−614.
(6) Knozinger, H. *Top. Catal.* **1998**, *6*, 107−110.
(7) Kobe, J. M.; Gonzalez, M. R.; Fogash, K. B.; Dumesic, J. A. *J. Catal.* **1996**, *164*, 459−466.
(8) Drago, R. S.; Kob, N. *J. Phys. Chem. B* **1997**, *101*, 3360−3364.
(9) Fogash, K. B.; Hong, Z.; Dumesic, J. A. *Catal. Lett.* **1998**, *56*, 85−93.
(10) Hong, Z.; Fogash, K. B.; Dumesic, J. A. *Catal. Today* **1999**, *51*, 269−288.
(11) Kim, S. Y.; Goodwin, J. G.; Galloway, D. *Catal. Lett.* **2000**, *64*, 1−8.
(12) Matsuhashi, H.; Shibata, H.; Nakamura, H.; Arata, K. *Appl. Catal., A* **1999**, *187*, 99−106.
(13) Hong, Z.; Fogash, K. B.; Watwe, R. M.; Kim, B.; Masqueda-Jimenez, B. I.; Natal-Santiago, M. A.; Hill, J. M.; Dumesic, J. A. *J. Catal.* **1998**, *178*, 489−498.
(14) Haw, J. F.; Nicholas, J. B.; Xu, T.; Beck, L. W.; Ferguson, D. B. *Acc. Chem. Res.* **1996**, *29*, 259−267.
(15) Tabora, J. E.; Davis, R. J. *J. Am. Chem. Soc.* **1996**, *118*, 12240−12241.
(16) Haase, F.; Sauer, J. *J. Am. Chem. Soc.* **1998**, *120*, 13503−13512.
(17) Babou, F.; Bigot, B.; Sautet, P. *J. Phys. Chem.* **1993**, *97*, 11501−11509.
(18) Davis, B. H.; Keogh, R. A.; Alerasool, S.; Zalewski, D. J.; Day, D. E.; Doolin, P. K. *J. Catal.* **1999**, *183*, 45−52.
(19) Zalewski, D. J.; Alerasool, S.; Doolin, P. K. *Catal. Today* **1999**, *53*, 419−432.
(20) Riemer, T.; Knozinger, H. *J. Phys. Chem.* **1996**, *100*, 6739−6742.
(21) Clingenpeel, T. H.; Wessel, T. E.; Biaglow, A. I. *J. Am. Chem. Soc.* **1997**, *119*, 5469−5470.
(22) Semmer, V.; Batamack, P.; Doremieux-Morin, C.; Vincent, R.; Fraissard, J. *J. Catal.* **1996**, *161*, 186−193.
(23) Sommer, J.; Habermacher, D.; Jost, R.; Sassi, A.; Stepanov, A. G.; Luzgin, M. V.; Freude, D.; Ernst, H.; Martens, J. *J. Catal.* **1999**, *181*, 265−270.
(24) Coster, D. J.; Bendada, A.; Chen, F. R.; Fripiat, J. J. *J. Catal.* **1993**, *140*, 497−509.
(25) Lunsford, J. H.; Sang, H.; Campbell, S. M.; Liang, C. H.; Anthony, R. G. *Catal. Lett.* **1994**, *27*, 305−314.
(26) Riemer, T.; Spielbauer, D.; Hunger, M.; Mekhemer, G. A. H.; Knozinger, H. *J. Chem. Soc., Chem. Commun.* **1994**, 1181−1182.

10.1021/ja0027721 CCC: $19.00
Published on Web 12/01/2000

better understand the structure, number, and strengths of these sites. One of the most commonly used measurements of the number and type of acid sites on solid catalysts is to adsorb the gas trimethylphosphine ($P(CH_3)_3$) onto the surface and then study the solid-state ^{31}P NMR spectra of this probe molecule. Lunsford and co-workers first demonstrated that the resonances of $P(CH_3)_3$ complexed to Lewis acid sites in zeolites are well-resolved from that due to $HP(CH_3)_3^+$, formed by adsorption onto Brønsted sites.[27,28] The use of $P(CH_3)_3$ in NMR probe molecule studies of zeolite solid acids has sometimes been criticized on the grounds that the inadvertent exposure of the sample to air results in the oxidation of the probe to trimethylphosphine oxide ($OP(CH_3)_3$). Some workers favor mixing catalysts with solid $OP(CH_3)_3$ to complex the surface sites with this alternative probe molecule.[29−31] $OP(CH_3)_3$ also complexes to both Lewis and Brønsted sites, but there has been disagreement as to the assignment of the resonances corresponding to these complexes in zeolites.

Previous studies of $P(CH_3)_3$ on sulfated zirconia catalyst[24−26] have revealed the unmistakable resonance of $HP(CH_3)_3^+$ near −2 ppm, two or more resonances in the region between −20 and −50 ppm (assigned to $P(CH_3)_3$ on Lewis sites), and a peak assigned to physisorbed $OP(CH_3)_3$ near +35 ppm. Adding complexity, other peaks have also been observed; the most troubling is a moderately sharp resonance near +27 ppm, the assignment of which has defied consensus. In the paper of Coster et al. this peak was assigned to $P(CH_3)_3$ adsorbed to an especially strong Lewis site,[24] while Lunsford et al. assigned this resonance to a complex between $P(CH_3)_3$ and an unidentified soft acid.[25] Knözinger and co-workers did not observe this peak at all in their study.[26] Also reported were broad, downfield resonances sometimes attributed to spinning sidebands of the $OP(CH_3)_3$ signal. By analogy to the zeolite studies, the formation of $OP(CH_3)_3$ on the surface of sulfated zirconia was attributed to inadvertent oxygen exposure.

This previous work suggests that the application of $P(CH_3)_3$ to the quantitative determination of Lewis and Brønsted acid sites on sulfated zirconia catalyst is contingent upon resolution of the assignment controversy of at least one and probably several peaks in the ^{31}P spectrum. For the present investigation, we have carefully evaluated several NMR probe molecules for the study of sulfated zirconia catalyst. Typically, each probe was studied as a function of loading (i.e., NMR surface titrations were carried out), and each was also studied on one or more crystalline forms of sulfur-free zirconia and sulfated zirconias prepared with diverse sulfur contents or by various procedures. We gave particular attention to two probes, $P(CH_3)_3$ and pyridine-^{15}N,[32] and we made extensive use of theoretical methods to aid in the assignment of the observed spectra.

We discovered that the oxidation of $P(CH_3)_3$ to $OP(CH_3)_3$ on sulfated zirconia is not the result of laboratory technique; instead, it reflects the oxidizing properties of the surface. Density functional calculations were used to optimize $P(CH_3)_3$ or $OP(CH_3)_3$ either alone, complexed to model adsorption sites, or derivatized to model reaction products that could plausibly be present on the catalyst surface. ^{31}P chemical shift tensors were then calculated using the GIAO-MP2 method.[33] Generally excellent agreement was obtained between theory and experiment for the uncontroversial assignments, but the theoretical ^{31}P chemical shifts of none of the acid−base adducts of either $P(CH_3)_3$ or $OP(CH_3)_3$ could account for the large signal we reproducibly observed at +27 ppm when high loadings of $P(CH_3)_3$ were absorbed onto sulfated zirconia. Drawing from analogy to the reactions of dimethyl chalconides on solid acids,[34,35] we considered the possibility that two $P(CH_3)_3$ molecules react with a Brønsted acid site to form tetramethylphosphonium ion, $P(CH_3)_4^+$. The theoretical and experimental ^{31}P shifts of this cation are in perfect agreement with this assignment. Formation of $P(CH_3)_4^+$ from $P(CH_3)_3$ on sulfated zirconia consumes a Brønsted acid site, and these are thus undercounted by integration of only the resonance due to $HP(CH_3)_3^+$. Stoichiometry requires that, for every mole of $P(CH_3)_4^+$ formed by disproportionation of $P(CH_3)_3$, there must also be a mole of $PH(CH_3)_2$, and the theoretical shift of $HPH(CH_3)_2^+$, −38 ppm, is near the center of the region assigned to $P(CH_3)_3$ on Lewis sites. This reaction thus leads to a 1-fold overcounting of Lewis sites and a 2-fold undercounting of Brønsted sites. Analogous theoretical studies of $OP(CH_3)_3$ reinforced the difficulty of assigning the adsorption state of this probe on the basis of chemical shift alone. Although $P(CH_3)_3$ is clearly a valuable probe molecule for the study of zeolite acidity, the oxidation and disproportionation reactions of this probe complicate its application to sulfated zirconia. After studying alternatives including $OP(CH_3)_3$, the ^{13}C and ^{15}N resonances of acetonitrile[36] or nitromethane,[37] acetone-2-^{13}C,[38,39] and ^{13}CO, we found that the careful application of pyridine-^{15}N provided a reliable method for measuring the concentrations of Lewis and Brønsted acid sites on sulfated zirconia. Oxidation of pyridine to pyridine-*N*-oxide does not occur on typical samples of sulfated zirconia, but it may occur on samples prepared by adsorption of large quantities of SO_3 onto zirconia.[40] Theoretical (GIAO-MP2) ^{15}N chemical shifts of models of pyridine complexed to Lewis and Brønsted acid sites were in excellent agreement with experimental values.

Experimental Section

Reagents. Pyridine-^{15}N (99% ^{15}N), acetone-2-^{13}C (99% ^{13}C), CO-^{13}C (99% ^{13}C), nitromethane-^{13}C (99% ^{13}C), nitromethane-^{15}N (99% ^{15}N), and acetonitrile^{15}N (99% ^{15}N) were purchased from Isotech. Trimethylphosphine oxide (>97%) was obtained from Alfa Aesar. Trimethylphosphine (97%), zirconyl chloride octahydrate (98%), sulfur dioxide (>99.9%), and sulfur trioxide (99%) were purchased from Aldrich.

Catalyst Preparation. Most of the results presented in this study were obtained for sulfated zirconia samples prepared using the standard, two-step method.[41,42] Zirconium hydroxide was prepared by hydrolysis

(27) Rothwell, W. P.; Shen, W.; Lunsford, J. H. *J. Am. Chem. Soc.* **1984**, *106*, 2452−2453.
(28) Lunsford, J. H.; Rothwell, W. P.; Shen, W. *J. Am. Chem. Soc.* **1985**, *107*, 1540−1547.
(29) Baltusis, L.; Frye, J. S.; Maciel, G. E. *J. Am. Chem. Soc.* **1986**, *108*, 7119−7120.
(30) Sutovich, K. J.; Peters, A. W.; Rakiewicz, E. F.; Wormsbecher, R. F.; Mattingly, S. M.; Mueller, K. T. *J. Catal.* **1999**, *183*, 155−158.
(31) Rakiewicz, E. F.; Peters, A. W.; Wormsbecher, F.; Sutovich, K. J.; Mueller, K. T. *J. Phys. Chem. B* **1998**, *102*, 2890−2896.
(32) Haw, J. F., Chuang, I.-S., Hawkins, B. L., and Maciel, G. E. *J. Am. Chem. Soc.* **1983**, *105*, 7206−7207.
(33) Gauss, J. *Chem. Phys. Lett.* **1992**, *191*, 614−620.
(34) Munson, E. J.; Haw, J. F. *J. Am. Chem. Soc.* **1991**, *113*, 6303−6305.
(35) Munson, E. J.; Kheir, A. A.; Haw, J. F. *J. Phys. Chem.* **1993**, *97*, 7321−7327.
(36) Haw, J. F.; Hall, M. B.; Alvarado-Swaisgood, A. E.; Munson, E. J.; Lin, Z.; Beck, L. W.; Howard, T. *J. Am. Chem. Soc.* **1994**, *116*, 7308−7318.
(37) Kheir, A. A.; Haw, J. F. *J. Am. Chem. Soc.* **1994**, *116*, 817−818.
(38) Xu, T.; Munson, E. J.; Haw, J. F. *J. Am. Chem. Soc.* **1994**, *116*, 1962−1972.
(39) Barich, D. H.; Nicholas, J. B.; Xu, T.; Haw, J. F. *J. Am. Chem. Soc.* **1998**, *120*, 12342−12350.
(40) Zhang, J.; Nicholas, J. B.; Haw, J. F. *Angew. Chemie* **2000**, *39*, in press.
(41) Hino, M.; Arata, K. *J. Chem. Soc., Chem. Commun.* **1980**, 851−852.

of zirconyl chloride ($ZrOCl_2 \cdot H_2O$) with aqueous ammonia (29.8%). Ammonia was slowly added to an aqueous solution of zirconyl chloride at room temperature. After stirring for 1 h, the precipitated gel (zirconium hydroxide) was washed with deionized water, filtered, and dried at 696 K for 24 hours. Sulfated zirconia samples with varying sulfur contents were prepared by controlled impregnation. Zirconium hydroxide fractions were soaked with 1 N sulfuric acid solution (3, 6, or 12 mL per 4 g of zirconium hydroxide) with stirring for 1 h at room temperature. The H_2SO_4-impregnated zirconium hydroxide samples were dried at 696 K in air for 24 h.

Several samples, designated SO_3/zirconia, were prepared by direct adsorption of SO_3 gas onto zirconia. SO_3 is an exceptionally noxious low-boiling liquid that oligomerizes upon prolonged standing. Solid SO_3 (Aldrich) was depolymerized by heating at 308 K, and milliter aliquots of the fuming liquid were transferred to vacuum line tubes within a nitrogen-purged glovebag. At room temperature, gaseous SO_3 was adsorbed onto zirconia which was previously calcined at 773 K.

Catalyst Characterization. Sulfur contents of the calcined catalysts were determined by elemental analysis. XRD patterns for zirconia and sulfated zirconia were obtained on a Seifert-Scintag PAD V automated diffractometer with Cu Kα radiation. The X-ray source was an anode operating at 40 kV and 30 mA with a copper target, filtered with nickel foil ($\lambda = 1.5418$ Å). Data were collected between 5 and 62° in 2φ with a step size of 0.04°. The scan rate was 1 K/min. The measured XRD patterns were compared with those in the JCPDS database. XRD measurements confirmed that our zirconia was primarily tetragonal after calcination up to 673 K, but monoclinic material was obtained after calcination at 873 K. In contrast, our sulfated zirconia was primarily tetragonal even after calcination at 873 K. Surface areas were determined by the nitrogen BET method and found to be typically 115 m^2/g for zirconia calcined at 773 K and 186 m^2/g for sulfated zirconia calcined at 873 K.

Sample Preparation for MAS NMR. All samples were prepared using an "ultra-shallow bed" CAVERN device similar to that shown in Figure 11 of ref 43. Most samples were prepared by the following procedure. Typically, 0.80 g of zirconia or sulfated zirconia was loaded into the CAVERN which was connected to a vacuum line. The catalyst was first calcined to a final temperature of 773 or 873 K with a heating rate of about 1.6 K/min. The catalyst was kept at the final temperature for 2 h under flowing air and then for 1 h in vacuo to a final pressure of less than 5×10^{-5} Torr. Adsorptions of volatile reagents were done at room temperature. The sample was loaded into a zirconia rotor within the CAVERN after adsorptions, and the rotor was capped.

Powdered trimethylphosphine oxide was mixed with calcined zirconia or sulfated zirconia and then loaded into the NMR rotor and capped within a glovebox under a nitrogen environment. All catalysts were used within 24 h of calcination. A Chemagnetics CMX-360 NMR spectrometer was used in this investigation.

Theoretical Methods. The geometries of all molecules and complexes were optimized using density functional theory at the B3LYP level[44] using the 6-311G* basis sets.[45] Frequency calculations were done to verify the optimized geometries were minima on the potential energy surface and to obtain the thermal corrections needed for the calculation of reaction enthalpies. Reported enthalpies correspond to conditions of 298.17 K and 1 atm. We used Gaussian98[46] for all of the optimizations and frequency calculations. The isotropic chemical shifts and chemical shift tensors were calculated using the GIAO method at the MP2 level of theory[33] and Ahlrich's TZPlarge basis set.[47] Chemical shifts are also reported at the RHF level to show the sensitivity of the results to electron correlation. In several cases we used a smaller hydrogen basis set (DZ) to make the calculation feasible. Absolute ^{31}P shieldings were converted to chemical shifts using the gas-phase isotropic value for PH_3 (−239 ppm) as a reference. Absolute ^{15}N shieldings were converted to chemical shifts by adjusting the calculated shift of nitrogen in NH_3 to the gas-phase experimental value of −399 ppm. The chemical shift calculations were performed using either Gaussian98 or ACES II.[48]

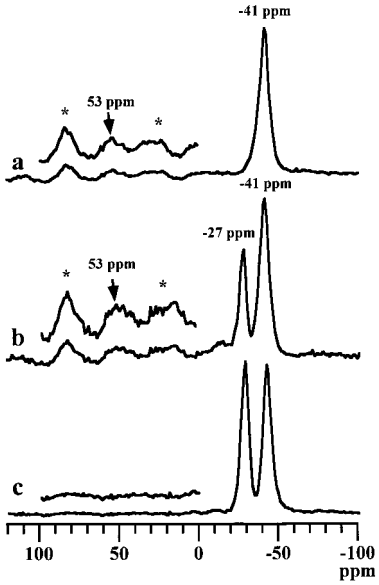

Figure 1. 145.6 MHz ^{31}P MAS NMR spectra of $P(CH_3)_3$ on pure zirconia which was calcined at various temperatures: (a) 673 K, (b) 773 K, and (c) 873 K under flowing air. Spectra were acquired at room temperature using single pulse excitation (Bloch decay) and proton decoupling. The pulse delay was 4 s, and 1000 scans were acquired.

Results

NMR Experiments Using $P(CH_3)_3$ and $OP(CH_3)_3$ Probes. We studied the ^{31}P MAS NMR spectra $P(CH_3)_3$ and $OP(CH_3)_3$ adsorbed onto several materials. Figure 1 reports ^{31}P MAS spectra of $P(CH_3)_3$ adsorbed onto sulfur-free zirconia samples calcined at various temperatures. For comparison, physisorbed $P(CH_3)_3$ is observed at ∼−62 ppm. When $P(CH_3)_3$ was absorbed onto zirconia calcined to 673 K, one intense resonance was observed at −41 ppm. This chemical shift is in the region commonly assigned to Lewis sites.[28] A second intense resonance at −27 ppm is also observed for samples calcined at 773 or 873 K. A broad, low-intensity signal centered at 53 ppm (and a series of spinning sidebands) is also seen for the two samples calcined at the lower temperatures.

Figure 2 reports ^{31}P MAS NMR spectra of various loadings of $P(CH_3)_3$ adsorbed onto a sulfated zirconia sample with a sulfur content of 4.6 wt %. The signals due to $P(CH_3)_3$ on Lewis sites are less well-defined on sulfated zirconia than on sulfur-free zirconia, and at a moderate loading (0.30 mmol/g) a single broad peak at ∼−30 ppm is observed in this spectral region. The signal at −2 ppm, unambiguously assigned to $HP(CH_3)_3^+$ by Lunsford,[27,28] is the most prominent peak at the lowest loading of $P(CH_3)_3$, 0.05 mmol/g. The downfield spinning sideband of the $HP(CH_3)_3^+$ resonance is also resolved near +17 ppm. The intensity of the $HP(CH_3)_3^+$ peak increases as the

(42) Corma, A.; Fornes, V.; Juan-Rajadell, M. I.; Nieto, J. M. L. *Appl. Catal., A* **1994**, *116*, 151−163.
(43) Xu, T.; Haw, J. F. *Top. Catal.* **1997**, *4*, 109−118.
(44) Becke, A. D. *J. Chem. Phys.* **1993**, *98*, 5648−5652.
(45) Hehre, W. J.; Radom, L.; Schleyer, P. v. R.; Pople, J. A. *Ab Initio Molecular Orbital Theory*; John Wiley & Sons: New York, 1986.
(46) Frisch, M. J.; Trucks, G. W.; Schlegal, H. B.; Gill, P. M. W.; Johnson, B. G.; Robb, M. A.; Cheeseman, J. R.; T. Keith; Petersson, G. A.; Montgomery, J. A.; Raghavachari, K.; Al-Laham, M. A.; Zakrzewski, V. G.; Ortiz, J. V.; Foresman, J. B.; Cioslowski, J.; Stefanov, B. B.; Nanayakkara, A.; Challacombe, M.; Peng, C. Y.; Ayala, P. Y.; Chen, W.; Wong, M. W.; Andres, J. L.; Replogle, E. S.; Gomperts, R.; Martin, R. L.; Fox, D. J.; Binkley, J. S.; Defrees, D. J.; Baker, J.; Stewart, J. P.; Head-Gordon, M.; Gonzalez, C.; Pople, J. A. *Gaussian 94*, revision B.2; Gaussian, Inc.: Pittsburgh, PA, 1995.
(47) Schafer, A.; Horn, H.; Ahlrichs, R. *J. Chem. Phys.* **1992**, *97*, 2571−2577.
(48) Stanton, J. F.; Gauss, J.; Watts, J. D.; Lauderdale, W. J.; Bartlett, R. J. *ACES II*, an ab initio quantum chemical program system.

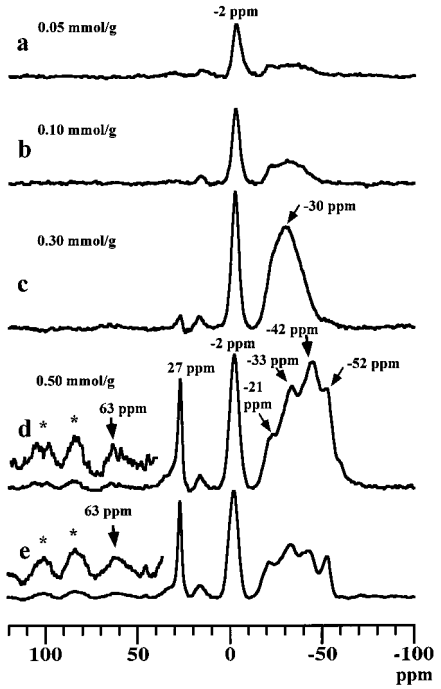

Figure 2. 145.6 MHz ^{31}P MAS NMR spectra (Bloch decay, 4 s pulse delay, 2000 scans) from a $P(CH_3)_3$ titration of sulfated zirconia (4.57 wt % S): (a) 0.05 mmol/g, (b) 0.10 mmol/g, (c) 0.30 mmol/g, (d) 0.50 mmol/g, and (e) ^{31}P CP/MAS NMR spectrum (2 ms contact time, 2 s pulse delay, and 4000 scans) of the sample with 0.50 mmol/g $P(CH_3)_3$.

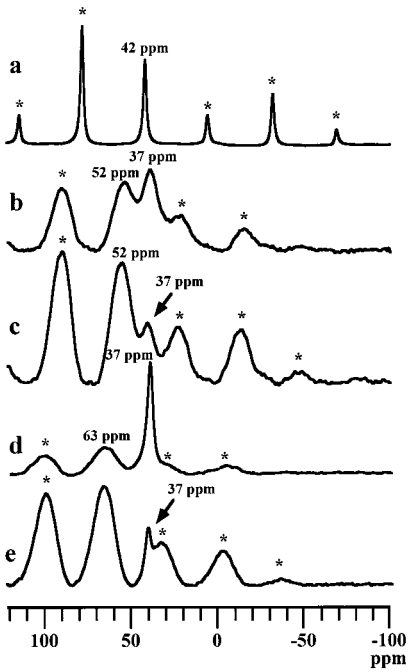

Figure 3. 145.6 MHz ^{31}P MAS NMR spectra (Bloch decay, 15 s pulse delay, 400 scans; cross polarization, 1 ms contact time, 2 s pulse delay, 4000 scans) of: (a) crystalline $OP(CH_3)_3$, Bloch decay; (b) $OP(CH_3)_3$ on pure zirconia, Bloch decay; (c) same as previous but with cross polarization; (d) $OP(CH_3)_3$ on sulfated zirconia, Bloch decay; (e) same as previous but with cross polarization.

loading is increased to 0.30 mmol/g, but it does not further increase at a loading of 0.50 mmol/g. Instead, the highest loading of $P(CH_3)_3$ affords a spectrum with an additional, sharp peak at +27 ppm. At this highest loading, additional structure is also seen in the region assigned to $P(CH_3)_3$ on Lewis sites, most prominently a peak at −42 and a shoulder at −52 ppm. In addition, a broad signal at +63 ppm (with associated spinning sidebands) is apparent at higher loadings. Figure 2 also compares the cross polarization and single-pulse (Bloch decay) spectra of the 0.50 mmol/g sample; although cross polarization alters the relative intensities of the several of the peaks, this method of excitation does not reveal additional signals or suggest a qualitatively different interpretation.

The use of $OP(CH_3)_3$ as an acidity probe was first proposed by Maciel;[29] we consider its use here because reports of $P(CH_3)_3$ on sulfated zirconia have suggested that some of the probe could have been oxidized. Figure 3 presents ^{31}P MAS NMR spectra of crystalline $OP(CH_3)_3$, $OP(CH_3)_3$ on zirconia calcined at 773 K, and $OP(CH_3)_3$ on sulfated zirconia. The CP/MAS spectra are compared with the Bloch decay spectra for the two latter cases. In the crystalline lattice, $OP(CH_3)_3$ has a ^{31}P isotropic shift of +42 ppm, and Figure 3 suggests that $OP(CH_3)_3$ physisorbed onto surfaces has a slightly different shift, +37 ppm. This resonance has no spinning sidebands and does not cross polarize effectively. The signals for $OP(CH_3)_3$ on the surfaces of zirconia and sulfated zirconia are not remarkably different; each is a broad signal with associated spinning sidebands. The isotropic peak is centered at 52 ppm for zirconia, and this shifts to 63 ppm for sulfated zirconia.

We also studied $P(CH_3)_3$ on zirconia samples treated with SO_3, a strong oxidant. Figure 4 shows that Brønsted sites are formed on zirconia by SO_3 treatment, but the $P(CH_3)_3$ in excess of that titrated by protons is oxidized to $OP(CH_3)_3$ on SO_3/zirconia, and no peaks are seen near −30 ppm for $P(CH_3)_3$ on Lewis sites. When 0.50 mmol/g of $P(CH_3)_3$ was adsorbed onto

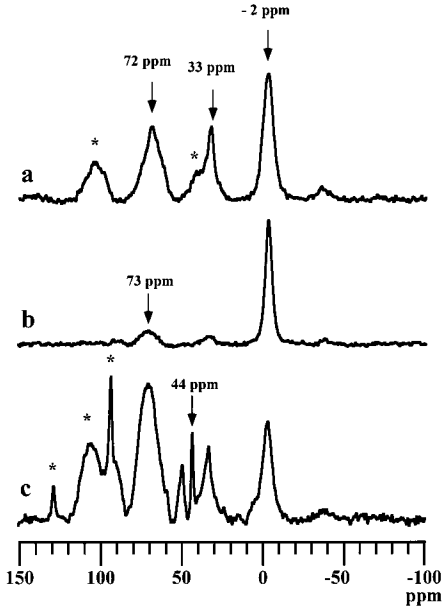

Figure 4. 145.6 MHz ^{31}P MAS NMR spectra of $P(CH_3)_3$ on samples of SO_3/zirconia (Bloch decay, 4 s pulse delay, 400 to 2000 scans): (a) 0.30 mmol/g on SO_3/zirconia (2.00 wt % S); (b) 0.17 mmol/g on SO_3/zirconia (4.57% S); and (c) 0.50 mmol/g on SO_3/zirconia (4.57% S).

zirconia treated with the highest loading of SO_3, so much $OP(CH_3)_3$ was formed that some of it phase separated as a solid (44 ppm).

Theoretical Studies of $P(CH_3)_3$ and $OP(CH_3)_3$ Probes. We used computational chemistry to model the complexes and reaction products that might form upon adsorption of $P(CH_3)_3$ and $OP(CH_3)_3$ on sulfated zirconia and to estimate the ^{31}P chemical shift tensors. The systems studied are listed in Table 1, which include the theoretical binding enthalpies and proton affinities. We used complexation with H^+ or HF to model

Table 1. B3LYP/6-311G* Binding Enthalpies and Proton Affinities (kcal/mol) for the Various Molecules and Complexes

complex	$\Delta H_{\text{Binding}}$
$HF{\cdot}P(CH_3)_3$	−10.1
$BF_3{\cdot}P(CH_3)_3$	−11.5
$SO_3{\cdot}P(CH_3)_3$	−24.6
$SO_2{\cdot}P(CH_3)_3$	−4.7
$HF{\cdot}OP(CH_3)_3$	−16.4
$BF_3{\cdot}OP(CH_3)_3$	−20.4
$SO_3{\cdot}OP(CH_3)_3$	−28.3
$SO_2{\cdot}OP(CH_3)_3$	−8.8
$BF_3{\cdot}PH(CH_3)_2$	−7.3
HF·Py	−13.5
BF_3·Py	−21.1
SO_3·Py	−21.9
SO_2·Py	−8.0
HF·PyN−O	−12.7
BF_3·PyN−O	−19.7
molecule	proton affinity
$P(CH_3)_3$	223.7
$OP(CH_3)_3$	217.5
$P(CH_3)_2$	213.4
Py	221.9
PyN−O	216.4

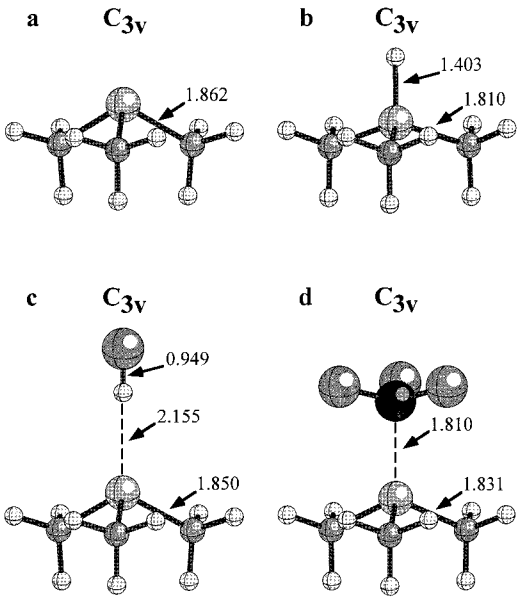

Figure 5. B3LYP/6-311G* optimized structures of: (a) $P(CH_3)_3$, (b) $HP(CH_3)_3^+$, (c) $HF{\cdot}P(CH_3)_3$, and (d) $BF_3{\cdot}P(CH_3)_3$. Symmetry point groups, selected bond lengths (Å) and bond angles are shown.

adsorption on Brønsted sites of greatly different strenghts,[39] and complexation with BF_3 to model adsorption on a Lewis site. Because SO_3, a strong oxidant, has previously been proposed as a species on the surface of sulfated zirconia,[16] we also considered the interaction of the probe molecules with SO_2 and SO_3. The most important objective of this study was to conclusively identify the species responsible for the +27 ppm signal (cf., Figure 2) and to asses its significance to acidity measurements. A secondary objective was to clarify the chemical shifts of $OP(CH_3)_3$ in acidic media.[29−31] An abbreviated study was carried out for the more straightforward case of the ^{15}N tensors of pyridine on sulfated zirconia, and this is reported below.

We first consider complexes of $P(CH_3)_3$ and $OP(CH_3)_3$ relevant to the chemistry and spectroscopy of these probes on sulfated zirconia. Figures 5 and 6 report representative optimized geometries for models used in the studies of $P(CH_3)_3$ and $OP(CH_3)_3$, respectively. Protonation of $P(CH_3)_3$ results in a P−H bond distance of 1.40 Å; for comparison, the calculated O−H distance for protonated $OP(CH_3)_3$, is 0.97 Å. Protonation of $OP(CH_3)_3$ lengthens the P−O distance by ∼0.1 Å. Table 1 shows that the B3LYP/6-311G* level of theory yields proton affinities of 223.7 and 217.5 kcal/mol for $P(CH_3)_3$ and $OP(CH_3)_3$, respectively. These values are in good agreement with the experimental proton affinties of 229.2 and 217.4 kcal/mol.[49] HF was used as a donor to model hydrogen bonding with a weak Brønsted acid. Figure 5 shows that the complexation of $P(CH_3)_3$ and HF produces a very long P−H distance (2.16 Å) and a P−F distance of 3.1 Å. Normal hydrogen bonding to the oxygen of $OP(CH_3)_3$ is observed in $HF{\cdot}OP(CH_3)_3$.

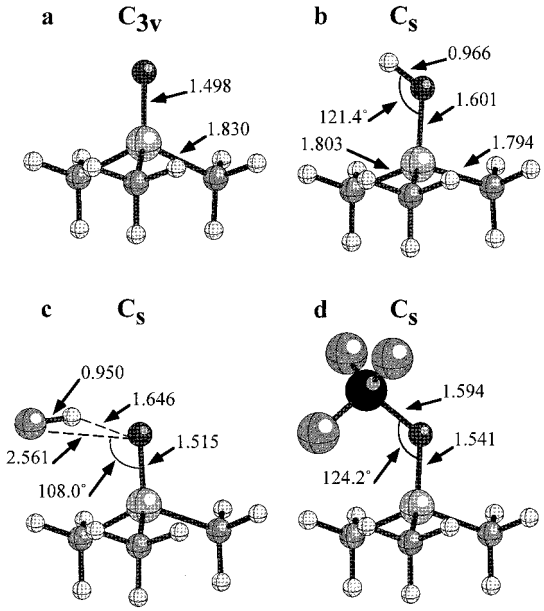

Figure 6. B3LYP/6-311G* optimized structures of: (a) $OP(CH_3)_3$, (b) $HOP(CH_3)_3^+$, (c) $HF{\cdot}OP(CH_3)_3$, and (d) $BF_3{\cdot}OP(CH_3)_3$. Symmetry point groups, selected bond lengths (Å) and bond angles are shown.

BF_3 was used as a simple Lewis site model; the stronger binding of this Lewis acid to $OP(CH_3)_3$ relative to $P(CH_3)_3$ was reflected in both the geometries and binding enthalpies. The optimized geometries of these sulfur oxide complexes (Supporting Information) and the theoretical binding enthalpies (Table 1) indicate that SO_3 binds more strongly than does SO_2.

^{31}P chemical shift calculations for all of the species discussed are summarized in Table 2. In many cases, the differences between RHF and MP2 values differ by 30 ppm or more, but the latter generally are in good or very good agreement with experiment. We will thus only discuss the MP2 values. The theoretical chemical shift of $P(CH_3)_3$, −50 ppm, showed one of the larger deviations from experiment with our referencing scheme. The gas-phase value is −63 ppm, and we observed a value for physisorbed $P(CH_3)_3$ of ∼−62 ppm. The calculated chemical shift for $HP(CH_3)_3^+$, −2 ppm, was identical to that which we observed for $P(CH_3)_3$ on sulfated zirconia.

Oxygen and nitrogen bases usually show hydrogen-bonding shifts upon complexation to weak or moderately strong acids that are intermediate between those of the free neutral and protonated species. Table 1 shows that $P(CH_3)_3$ is anomalous; the shift of $HF{\cdot}P(CH_3)_3$ is *upfield* of $P(CH_3)_3$. However, the geometry of this complex makes it clear that $P(CH_3)_3$ is not a conventional hydrogen-bond acceptor. The calculated ^{31}P iso-

(49) The experimental proton affinity values reported here are the most recent values or the values with the smallest uncertainties listed in the NIST Chemistry WebBook (http://webbook.nist.gov/chemistry/).

Table 2. ^{31}P Chemical Shift Data Calculated at MP2/TZP (large) for the $P(CH_3)_3$ and $OP(CH_3)_3$ Models Described in the Text[a]

model	δ_{iso}	δ_{11}	δ_{22}	δ_{33}	δ_{CSA}	η
PH_3	−239	−203	−257	−257	−54	0.00
$P(CH_3)_3$	−50	−34	−59	−59	−24	0.00
$HP(CH_3)_3^+$	−2	38	−22	−22	−60	0.00
$HF{\cdot}P(CH_3)_3$	−54	−25	−68	−68	−43	0.00
$BF_3{\cdot}P(CH_3)_3$	−31	−4	−44	−44	−40	0.00
$OP(CH_3)_3$	34	112	112	−122	234	0.00
$HOP(CH_3)_3^+$	111	154	148	32	118	0.08
$HF{\cdot}OP(CH_3)_3$	53	119	116	−76	193	0.02
$BF_3{\cdot}OP(CH_3)_3$[b]	72	117	116	−17	134	0.01
$SO_3{\cdot}P(CH_3)_3$	13	14	14	11	3	0.00
$SO_3{\cdot}OP(CH_3)_3$[c]	67	119	113	−31	147	0.05
$SO_2{\cdot}P(CH_3)_3$	−42	−23	−50	−53	−29	0.16
$SO_2{\cdot}OP(CH_3)_3$	39	107	90	−79	178	0.15
$SP(CH_3)_3$	41	103	103	−82	185	0.00
$P(CH_3)_4^+$	26	26	26	26	0	0.00
$PH(CH_3)_2$	−89	−48	−83	−136	70	−0.75
$HPH(CH_3)_2^+$	−38	8	−31	−90	78	−0.75
$BF_3{\cdot}PH(CH_3)_2$	−62	−25	−67	−95	−56	0.75

[a] All parameters but η (dimensionless) are in ppm. [b] For H-atoms the DZP basis set was used instead of TZP (large) to conform to program limitations. [c] For both C- and H-atoms the DZP basis set was used instead of TZP (large) to conform to program limitations.

tropic shift of the Lewis site model $BF_3{\cdot}P(CH_3)_3$, −31 ppm, falls neatly between the two peaks seen for adsorption of $P(CH_3)_3$ onto zirconia calcined at higher temperatures (Figure 1).

$OP(CH_3)$ was more conventional in regard to hydrogen bonding; the theoretical ^{31}P isotropic shift of $HF{\cdot}OP(CH_3)_3$ (53 ppm) is intermediate between those of the free base (34 ppm) and $HOP(CH_3)_3^+$ (111 ppm). Unfortunately, this wide range of shifts for $OP(CH_3)$ interacting with Brønsted acids overlaps with that for Lewis sites; we calculated values of 72 ppm for $BF_3{\cdot}OP(CH_3)_3$ and 67 ppm for $SO_3{\cdot}OP(CH_3)_3$. Thus, like acetone-2-^{13}C[38,39] and several other commonly used NMR acidity probes, there is overlap of the isotropic shift ranges for Brønsted and Lewis sites, and a universal classification of Brønsted and Lewis sites based on the ^{31}P shift of $OP(CH_3)_3$ is not possible.

Examining the experimental ^{31}P NMR spectra in Figure 2, one notes a broad isotropic signal at 63 ppm with a series of associated spinning sidebands. We assign this signal to $OP(CH_3)_3$ complexed to acid sites on sulfated zirconia, but the breadth of this signal and the overlapping ranges for Brønsted and Lewis sites argues against a more specific assignment. One oxidizing species previously proposed to exist on the surface of sulfated zirconia is SO_3; our theoretical enthalpies show that reaction between this species and trimethylphosphine is very exothermic:

$$SO_3{\cdot}P(CH_3)_3 \rightarrow SO_2{\cdot}OP(CH_3)_3 \quad \Delta H_{rxn} = -53.8 \text{ kcal/mol}$$

The binding of SO_2 to $OP(CH_3)_3$ is relatively weak, only −8.8 kcal/mol (Table 1), and SO_2 would likely be displaced by either a Brønsted site or a stronger Lewis site provided by the surface.

None of the species discussed thus far suggest an explanation for the moderately sharp peak at +27 ppm. We considered a number of other possible reaction products between $P(CH_3)_3$ and sources of oxygen and sulfur. The theoretical ^{31}P shift tensor for $SP(CH_3)_3$ is reported in Table 2, but this and other such species (not shown) failed to account for the +27 ppm signal. Progress was made when we considered the following reaction:

$$P(CH_3)_3 + HP(CH_3)_3^+ \rightarrow P(CH_3)_4^+ + PH(CH_3)_2$$

The theoretical enthalpy of the above reaction is −9.2 kcal/mol. The experimental chemical shift of $P(CH_3)_4^+$ is 25 ppm in solution, whereas we calculated a theoretical value of 26 ppm. The T_d symmetry of this cation requires that all three principal components of the ^{31}P chemical shift tensor be identical, which is reflected in the moderately sharp line with no spinning sidebands observed by us and others.[24,25] Verification of this assignment was achieved by the rational synthesis of $P(CH_3)_4^+$ on the zirconia surface. We coadsorbed $P(CH_3)_3$ and $^{13}CH_3Br$ onto zirconia, and obtained the ^{31}P and ^{13}C spectra shown in Figure 7. The ^{13}C spectrum shows that methyl bromide reacted in two ways. Reaction with nucleophilic base sites produced surface methoxy species at 54 ppm, similar to those seen in the reaction of methyl halides on basic, metal-exchanged zeolites.[50] A second, sharp peak was observed at 7 ppm. For comparison, the calculated ^{13}C chemical shifts of $P(CH_3)_3$ and $P(CH_3)_4^+$ were 17.8 and 12.1 ppm, respectively. The ^{31}P spectrum was conclusive; while some of the $P(CH_3)_3$ was absorbed on Lewis sites, much was alkylated to form $P(CH_3)_4^+$ at 27 ppm. The line widths of the pertinent signals in the ^{31}P and ^{13}C spectra were too broad for us to resolve scalar coupling between these nuclei.

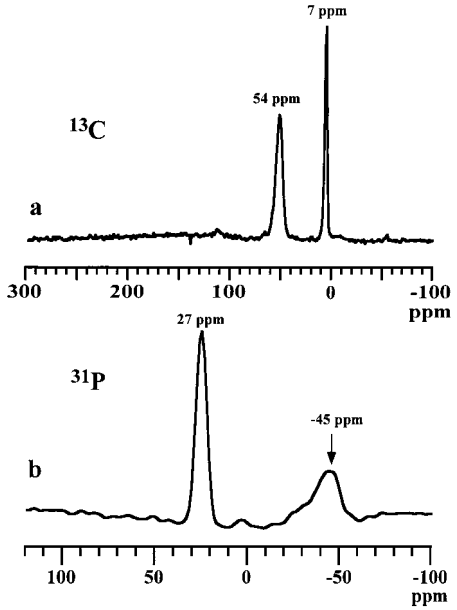

Figure 7. MAS NMR spectra of $P(CH_3)_3$ and $^{13}CH_3Br$ coadsorbed onto zirconia: (a) 50.1 MHz ^{13}C CP/MAS spectrum, 2 ms contact time, 1 s pulse delay, 4000 scans; (b) 145.6 MHz ^{31}P MAS NMR spectrum, 12 s pulse delay, and 8000 scans.

The formation of $P(CH_3)_4^+$ on sulfated zirconia by the disproportionation of $P(CH_3)_3$ requires that a stoichiometric quantity of $PH(CH_3)_2$ also form. The theoretical shift of $PH(CH_3)_2$, −89 ppm (Table 2) is in good agreement with the literature value, but our experimental spectra of $P(CH_3)_3$ on sulfated zirconia (Figure 2) do not reveal any peaks this far upfield. However, $PH(CH_3)_2$ also complexes to Brønsted and Lewis sites. The theoretical chemical shifts for $HPH(CH_3)_2^+$ and $BF_3{\cdot}PH(CH_3)_2$ were −38 and −62 ppm, respectively. Close inspection of Figure 2 shows that the formation of the +27 ppm signal is accompanied by a nearly equal intensity signal at ∼−42 ppm. We assign the −42 ppm resonance to $HPH(CH_3)_2^+$. The calculated proton affinity of $PH(CH_3)_2$ is 213.4 kcal/mol (cf., 218.0 experiment), and it is reasonable that this molecule will be protonated on a solid acid catalyst.

NMR Experiments Using Pyridine-^{15}N as a Probe. NMR titrations of Brønsted and Lewis sites on solid acids using

(50) Murray, D. K.; Chang, J. W.; Haw, J. F. *J. Am. Chem. Soc.* **1993**, *115*, 4732−4741.

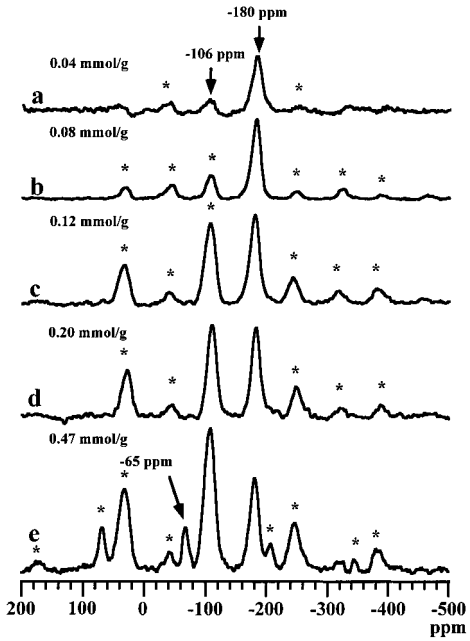

Figure 8. 36.5 MHz ^{15}N CP/MAS spectra of pyridine-^{15}N titrating sulfated zirconia (4.57 wt % S): (a) 0.04 mmol/g, (b) 0.08 mmol/g, (c) 0.12 mmol/g, (d) 0.20 mmol/g, and (e) 0.47 mmol/g. All spectra were acquired at 123 K with a contact time of 5 ms, a pulse delay of 2 s, and 1000−1200 transients.

pyridine-^{15}N have been previously described,[32] but this approach has been little used because the probe can undergo fast chemical exchange on some catalysts at room temperature and because the sensitivity of ^{15}N is low, even with complete isotopic enrichment. We addressed these problems by working out the experimental conditions for ^{15}N CP/MAS spectra of pyridine on sulfated zirconia at a temperature of 123 K, a value low enough to ensure slow-exchange spectra and improve sensitivity through improved cross polarization efficiency, the Boltzman factor, and reduced coil noise. A variable contact time experiment established an optimal contact time of 5 ms, which yielded quantitative results for both Brønsted and Lewis sites. Figure 8 reports a pyridine-^{15}N NMR titration of the same sulfated zirconia sample studied in Figure 2 using $P(CH_3)_3$. A peak at −180 ppm, expected for pyridine on a Brønsted site, is most prominent with the lower loadings and reaches a maximum when ∼0.12 mmol/g is adsorbed. Pyridine-^{15}N shows one signal, at −101 ppm on sulfur-free zirconia, and this Lewis acid signal is seen at −106 ppm on sulfated zirconia. The Brønsted site is preferred to the Lewis site with a limiting amount of pyridine, and the latter is not fully titrated until ∼0.47 mmol/g of pyridine is adsorbed. At this highest loading studied a small amount of excess titrant is apparent through the peak at −65 ppm.

From the integrated intensities of the isotropic peaks and associated spinning sidebands in Figure 8 (0.47 mmol/g spectrum) we determined that this particular sample of sulfated zirconia has 0.099 mmol/g Brønsted sites and 0.29 mmol/g Lewis sites that are accessible to pyridine. Given that this sample contained 1.4 mmol/g sulfur, only ∼7% of sulfurs correspond to Brønsted acid sites that protonate pyridine on this catalyst. We used the pyridine-^{15}N probe to explore the effects of catalyst composition and treatment on the relative number of Brønsted sites. Figure 9 shows that the addition of small amounts of water, for example, 0.06 mmol/g, to this same catalyst produced a corresponding increase in the number of Brønsted sites, but Brønsted sites strong enough to protonate pyridine were not formed by adsorption of water to sulfur-free zirconia. We also found that the number of Brønsted sites also depends on the sulfur loading for otherwise identical preparations (results reported in Supporting Information).

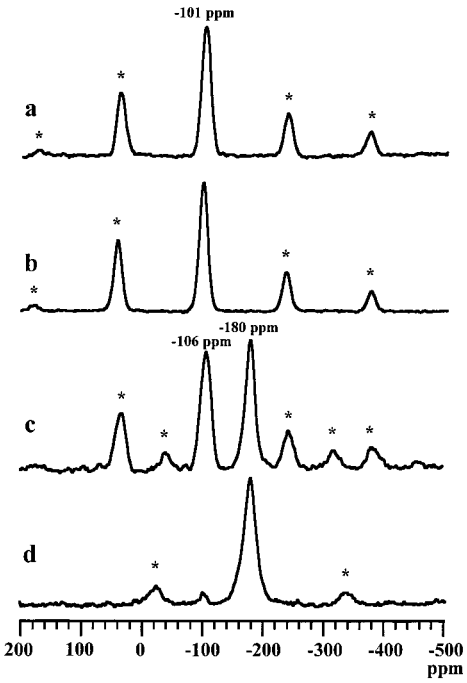

Figure 9. 36.5 MHz ^{15}N CP/MAS NMR spectra of 0.12 mmol/g of pyridine-^{15}N on various samples: (a) zirconia calcined at 773 K, (b) as previous but treated at room temperature with 0.06 mmol H_2O, (c) sulfated zirconia (4.57% S), and (d) as previous but treated at room temperature with 0.06 mmol H_2O. All spectra were acquired at 123 K with a contact time of 5 ms, pulse delay of 2 s, and 1000−1200 transients.

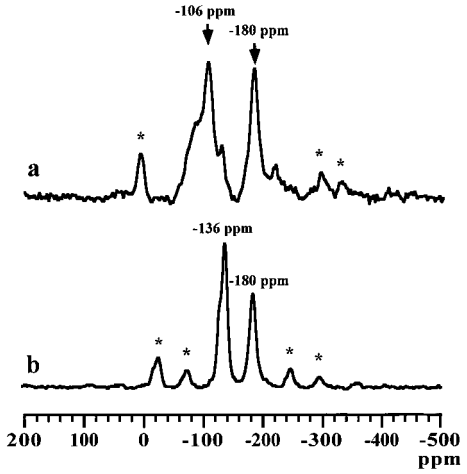

Figure 10. 36.5 MHz ^{15}N CP/MAS NMR spectra of 0.20 mmol/g pyridine-^{15}N on samples of SO_3/zirconia: (a) 2.00 wt % S and (b) 4.57 wt % S. All spectra were acquired at 123 K with a contact time of 4 ms, a pulse delay of 2 s, and 8000 scans.

We did not encounter any assignment difficulties with pyridine-^{15}N as a probe until we adsorbed this molecule onto catalysts prepared by direct adsorption of SO_3 on zirconia.[40] Figure 10 shows that adsorption of 0.2 mmol/g of pyridine-^{15}N onto SO_3/zirconia with only 2.0% final sulfur produces a spectrum similar to conventional sulfated zirconia with both Brønsted (−180 ppm) and Lewis (−106 ppm) sites, but with a catalyst prepared with a much higher SO_3 loading, the familiar Lewis site is replaced with a peak at −136 ppm.

Table 3. ^{15}N Chemical Shift Data Calculated at MP2/TZP (large) for the Pyridine Models Described in the Text[a]

model	δ_{iso}	δ_{11}	δ_{22}	δ_{33}	δ_{CSA}	η
NH_3	−399	−369	−414	−414	−46	0.00
Py	−70	201	25	−436	549	0.48
H Py^+	−194	−33	−186	−362	252	0.91
HF·Py	−95	121	14	−421	489	0.33
BF_3·Py	−125	8	2	−384	389	0.03
SO_3·Py	−92	72	−1	−346	382	0.29
SO_2·Py	−69	189	11	−406	506	0.53
PyN-O	−73	31	22	−273	299	0.04
PyN-OH^+	−142	−7	−150	−270	−204	0.89
HF·PyPyN-O	−75	48	10	−283	312	0.18
BF_3·PyN-O	−108	31	−67	−287	269	0.55

[a] All parameters but η (dimensionless) are in ppm.

Theoretical Studies of the Pyridine-^{15}N Probe. As an aid to the interpretation of the spectra of pyridine-^{15}N on acidic catalysts we studied pyridine complexed to Brønsted and Lewis acids, as well as complexes of pyridine-*N*-oxide and protonated analogues. These structures were largely unremarkable and are reported in the Supporting Information. Calculated proton affinitites for pyridine (221.9 kcal/mol) and pyridine-*N*-oxide (216.5 kcal/mol, Table 1) compare to experimental values of 222 and 220.7 kcal/mol, which again indicates that the B3LYP/6-311G* level of theory provides reasonable energetics. Table 3 reports theoretical ^{15}N chemical shifts for the complexes of pyridine. The isotropic ^{15}N chemical shift of free pyridine (−70 ppm) is shifted upfield by hydrogen bonding (−95 ppm for the HF complex). Protonated pyridine was predicted to have a chemical shift of −194 ppm, which might be compared to the value of −180 ppm for Brønsted sites on sulfated zirconia. Using BF_3 to model a Lewis site gave a ^{15}N chemical shift of −125 ppm for pyridine, which is ∼20 ppm farther upfield than the chemical shift usually attributed to Lewis site adsorption on sulfated zirconia. In addition, the predicted ^{15}N chemical shift for the SO_3·Py complex (−92 ppm) cannot be equated to the −136 ppm peak seen for pyridine on zirconia treated with high loadings of SO_3.

We therefore considered the possibility that pyridine could be oxidized on the SO_3/zirconia surface by analogy to the exothermic conversion of SO_3·$P(CH_3)_3$ to SO_2·$OP(CH_3)_3$. However, theory shows that the following reaction is slightly endothermic.

$$SO_3\cdot Py \rightarrow SO_2\cdot Py\text{-}N{-}O \quad \Delta H_{rxn} = +4.6 \text{ kcal/mol}$$

Nevertheless, we considered the possibility that pyridine-*N*-oxide could form under more strongly oxidizing conditions, which we assume could exist on the surface. Pyridine-*N*-oxide has a ^{15}N chemical shift (−73 ppm) similar to that of pyridine. Complexation of pyridine-*N*-oxide with HF has only a minor effect on the chemical shift (−75 ppm), whereas protonation gives a chemical shift of −142 ppm. However, the theoretical results predict that oxidation of pyridine to pyridine-*N*-oxide, followed by protonation, would give a peak at −142 ppm, which may correspond to the experimental value (−136 ppm).

Other Probe Molecules on Sulfated Zirconia. Acetone-2-^{13}C, acetonitrile-^{15}N, acetonitrile-^{13}C, and ^{13}CO were also evaluated as acidity probes on some of the catalysts studied here. None appeared to be especially promising. On sulfated zirconia, acetone underwent aldol condensation at room temperature and dehydration and cracking reactions at elevated temperature (^{13}C spectra reported in Supporting Information). The only miscellaneous result of any significance was obtained for nitromethane; Figure 11 reports ^{15}N and ^{13}C spectra of this probe on sulfated zirconia. On basic surfaces, nitromethane deprotonates to form the *aci* anion,[37] with an ^{15}N shift of −80 ppm and a ^{13}C shift of 114 ppm. Figure 11 demonstrates that basic sites exist on sulfated zirconia.

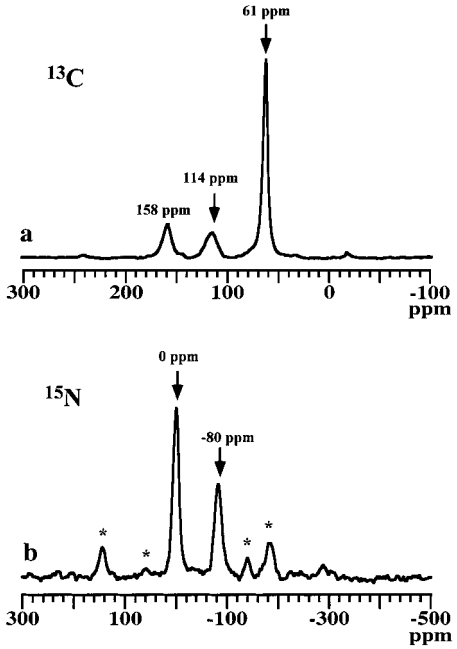

Figure 11. CP/MAS NMR spectra of nitromethane on sulfated zirconia: (a) ^{13}C spectrum measured at 298 K, (b) ^{15}N spectrum measured at 123 K.

Discussion

The application of $P(CH_3)_3$ as a probe molecule for the acid sites of sulfated zirconia is complicated by the oxidation of this probe by the surface and by the disproportionation to form $P(CH_3)_4^+$ and $PH(CH_3)_2$. The assignment of the moderately sharp peak at +27 ppm to $P(CH_3)_4^+$ is conclusive and significant. Disproportionation of $P(CH_3)_3$ consumes a Brønsted site, and the coproduct $PH(CH_3)_2$ is protonated to yield a signal in the spectral region assigned to $P(CH_3)_3$ on Lewis sites. Disproportionation is favored at higher loadings of $P(CH_3)_3$, but for our catalyst sufficiently high loadings were needed to titrate all acid sites so that $P(CH_3)_4^+$ formation was unavoidable (Figure 2).

A very small amount of $P(CH_3)_4^+$ can be discerned in a previous study of acid sites in a zeolite,[28] but this reaction occurs readily on sulfated zirconia. This could reflect differences in the acid strengths of the two materials. The analogous disproportionation reaction of dimethyl ether produces trimethyloxonium, $O(CH_3)_3^+$, and methanol.[34,35] The extent of this reaction on various zeolites correlates with commonly held views of relative acidic strength.[51] Thus, the +27 ppm peak could be valuable as a diagnostic of acid strength.

The adsorption of $P(CH_3)_3$ onto some zirconia samples and probably all sulfated zirconia samples produces some $OP(CH_3)_3$ as a result of the inherent oxidizing power of surface sites. $OP(CH_3)_3$ formation was especially pronounced on SO_3-treated zirconia samples. The assignment of the spectra of $OP(CH_3)_3$ on solid acids has been and remains problematic. Phase-separated, solid $OP(CH_3)_3$ has an isotropic shift of 42 ppm, and we observe physisorbed $OP(CH_3)_3$ as a sharp line at 37 ppm. There are no universal chemical shift ranges for Brønsted and

(51) Haw, J. F.; Xu, T.; Nicholas, J. B.; Goguen, P. W. *Nature* **1997**, *389*, 832−835.

Lewis sites with this probe molecule, although the assignment may be straightforward for specific acids. $OP(CH_3)_3$ is observed at 52 ppm on the Lewis sites of zirconia, and modeling suggests that Lewis complexes can be at least as far downfield as 72 ppm. The assignment of $OP(CH_3)_3$ on Brønsted sites is problematic, and this can best be understood by comparison with trimethylphosphine. $P(CH_3)_3$ has an exceptionally high gas-phase proton affinity, 229.2 kcal/mol, and it does not form traditional hydrogen-bonded complexes as do oxygen and nitrogen bases. Thus, proton transfer to $P(CH_3)_3$ is essentially an all-or-nothing event, and $HP(CH_3)_3^+$ has a very narrow chemical shift range on a wide variety of acidic catalysts. The observation of appreciable $^1H-^{31}P$ through-bond scalar and through-space dipolar couplings provided Lunsford et al. with an unambiguous assignment for $HP(CH_3)_3^+$.[27]

In contrast, $OP(CH_3)_3$ has a proton affinity of 217.4 kcal/mol and forms conventional hydrogen bonds with Brønsted acids. The combination of lower base strength and hydrogen bonding results in a wide range of ^{31}P chemical shifts for $OP(CH_3)_3$ complexed with Brønsted acids. While this might be useful in that the observed shift could possibly be correlated to acid strength, it contributes to assignment problems. Incomplete proton transfer severely attenuates the (theoretical) shift of 111 ppm for $HOP(CH_3)_3^+$, and in the case of sulfated zirconia, the observed value of 63 ppm is only marginally different from the 52 ppm signal on the Lewis sites of zirconia, as the signal is broad in each case.

The application of pyridine-^{15}N to sulfated zirconia was instrumentally more challenging in that the measurements were made at a low temperature; however, the interpretation of the results was straightforward. The proton affinity of pyridine, 222 kcal/mol, is intermediate between those of $P(CH_3)_3$ and $OP(CH_3)_3$. The pyridine nitrogen on the Brønsted sites of sulfated zirconia is seen at -180 ppm, very close to the theoretical value for the isolated protonated molecule, -194 ppm. It is conceivable that there could be some weak solid acids where incomplete proton transfer to pyridine (cf., the theortical results for Py·HF) creates the possibility of overlap between Brønsted and Lewis ranges, but we found no evidence of ambiguity for sulfated zirconia. At the highest loading studied we observed a sharp peak at -65 ppm which compares well with the theoretical shift of free pyridine, -70 ppm. This isotropic peak also has associated spinning sidebands, indicating restricted motion, and we assign this species to frozen, rather than physisorbed, pyridine. The observation of a clearly resolved peak for excess base is a useful measure of the endpoint in the NMR titration of a surface.

For the specific sulfated zirconia catalyst studied in the greatest detail, the pyridine-^{15}N measurement determined 0.099 mmol/g of Brønsted sites and 0.29 mmol/g Lewis sites. From the spectral assignments reported above, is it possible to reconcile the $P(CH_3)_3$ measurement with the pyridine result? We selected the Bloch decay spectrum in Figure 2 corresponding to a $P(CH_3)_3$ loading of 0.50 mmol/g. Since this spectrum does not show a peak for physisorbed $P(CH_3)_3$, there is at least one minor discrepancy in that pyridine was very slightly in excess at 0.47 mmol/g. A larger problem was posed by our inability to conclusively identify the acid sites on which the $OP(CH_3)_3$ was adsorbed; we therefore neglected the 63 ppm signal and its spinning sidebands which collectively accounted for 7.9% of the total integrated intensity. We integrated the three remaining major peaks in the ^{31}P spectrum, the 27 ppm resonance due to $P(CH_3)_4^+$ ($I_{27\ ppm}$), that at -2 ppm due to $HP(CH_3)_3^+$ ($I_{-2\ ppm}$), and the collection of poorly resolved signals between -12 ppm and -80 ppm, which is conventionally assigned to $P(CH_3)_3$ on Lewis sites (I_{Lewis}). Consideration of the balanced chemical reaction for $P(CH_3)_4^+$ formation, as discussed above, suggests that the "true" Lewis sites are given by $I_{Lewis} - I_{27\ ppm}$ while the Brønsted sites should be better measured by $I_{-2\ ppm} + 2I_{27\ ppm}$.

This interpretation of the ^{31}P spectrum of $P(CH_3)_3$ gives a measure of the Lewis site concentration of 0.28 mmol/g, in excellent agreement with the value of 0.29 mmol/g from the ^{15}N spectrum of pyridine-^{15}N. However, measuring the Brønsted sites as $I_{-2\ ppm} + 2I_{27\ ppm}$ yields a value of 0.18 mmol/g, that is almost twice the value of 0.099 mmol/g determined using pyridine. The two most reasonable explanations for this discrepancy are steric effects and differences in base strengths, and it is probable that both factor in the number of Brønsted sites capable of protonating a given probe. Detailed modeling of steric effects is not possible, because far too little is known about the topology of the surface to permit such. $P(CH_3)_3$ is more basic than pyridine, with proton affinities of 229.2 and 222 kcal/mol, respectively; however, we earlier concluded that $PH(CH_3)_2$ is protonated on the sulfated zirconia surface, and the proton affinity of that base, formed in the disproportionation of $P(CH_3)_3$, is only 208.0 kcal/mol. $PH(CH_3)_2$ is smaller than $P(CH_3)_3$, and may be able to access some stronger, sterically less-accessible sites. Note that such a discrepancy is much less likely to be encountered in analogous studies of medium- or large-pore zeolites, where the strength of Brønsted sites are believed to be more nearly uniform and the pore size does not provide much steric discrimination for $P(CH_3)_3$ against pyridine.

Conclusions

We must conclude that on sulfated zirconia, both $P(CH_3)_3$ and pyridine provide *operational* measures of the number of Brønsted sites, and this must be also true for the number of Lewis sites, even though the probes agree on the latter measure. The value of any such measure lies in comparative studies as in Figures 9 and 10, where the same measurement is applied to samples varied in a systematic way (e.g., before and after water treatment). In the case of sulfated zirconia, we favor and endorse the use of pyridine, because the spectra, while more difficult to measure, are more straightforward to interpret. Those Brønsted acid sites that are active in the low-temperature chemistry of hydrocarbons are presumably the strongest ones present. Simple olefins have proton affinities ~40 kcal/mol lower than that of pyridine, and it seems certain that even the pyridine number greatly over-counts the absolute concentration of Brønsted sites that are active for hydrocarbon catalysis at low temperatures.

This study has revealed important details about the acidity of sulfated zirconia catalysts. The number of Brønsted acid sites on sulfated zirconia that protonate pyridine is far lower than the number of sulfurs. However, for a commonly used method of catalyst preparation, there is a simple correlation between the sulfur content and the concentration of Brønsted sites. Even for the catalyst with the highest sulfur content studied, the concentration of Lewis sites exceeds that of Brønsted sites. The concentration of Brønsted sites on sulfated zirconia is sensitive to the addition of water, but water treatment of sulfur-free zirconia does not introduce strong Brønsted acidity. A recent theoretical investigation concluded that one of the possible forms of sulfur on sulfated zirconia is a form of adsorbed SO_3.[16] We found that sulfated zirconia has an ability to oxidize $P(CH_3)_3$ that is not shared by sulfur-free zirconia activated to a comparable temperature. SO_3 is a plausible surface species on our materials in that it is a strong oxidant that reacts with water to form sulfuric acid.

Catalysts prepared by direct adsorption of SO_3 onto zirconia had some Brønsted sites,[40] but the oxidation of $P(CH_3)_3$ on these materials was more severe than that on conventional sulfated zirconia samples with comparable sulfur contents. Pyridine-^{15}N also showed a unique peak on samples of zirconia treated with a very high loading of SO_3. The most probable assignment of this resonance is pyridine-*N*-oxide on a Brønsted site, although oxidation of pyridine by monomeric SO_3 was predicted to be slightly endothermic in the gas phase.

Sulfated zirconia catalyst is very complex material that also has basic sites on the surface, as confirmed by deprotonation of nitromethane. The constellation of Brønsted and Lewis acidity, Brønsted basicity, and oxidizing power described here can be little comfort in the search for simple mechanistic models of chemistry on this catalyst.

Acknowledgment. J.F.H. is supported by the National Science Foundation (CHE-9996109, and CTS-9996109) and the U.S. Department of Energy (DOE) Office of Basic Energy Sciences (BES) (Grant No. DE-FG03-93ER14956). J.B.N. is funded by the Department of Energy (DOE) Office of Science. Computer resources were provided by the National Energy Research Supercomputer Center (NERSC), Berkeley, CA, by the Molecular Science Computing Facility (MSCF) at PNNL, and by the National Center for Supercomputing Applications (NCSA). Pacific Northwest National Laboratory is a multipurpose national laboratory operated by Battelle Memorial Institute for the U.S. DOE.

Supporting Information Available: Seven figures and two tables reporting results referred to in the text (PDF). This material is available free of charge via the Internet at http://pubs.acs.org.

JA0027721